Petroleum and Coal

Article **Open Access**

Parametric Investigation of Empty Fruit Bunch Gasification using Response Surface Methodology

Girma T. Chala[1], Chin L. Liew[2], Shaharin A. Sulaiman[3], Muddasser Inayat[3], Fiseha M. Guangul[4]*

[1] *International College of Engineering and Management, Muscat, Oman*
[2] *INTI International University, Nilai, Malaysia*
[3] *Department of Mechanical Engineering, Universiti Teknologi PETRONAS, 32610 Bandar Seri Iskandar, Perak Darul Ridzuan, Malaysia*
[4] *Middle East College, Muscat, Oman*

Received June 21, 2021; Accepted January 14, 2022

Abstract

Nowadays emissions of greenhouse gases from fossil fuels have become a serious environmental problem. Besides, an ever-growing demand for energy sources, which is in dissonance with a limited supply of fossil fuels, has also become another related concern. Subsequently, alternative energy sources have received dramatic attention in an effort to reduce the usage of fossil fuels and increase its share in the future energy production. This paper is, therefore, aimed at investigating the potential usage of Empty Fruit Bunch (EFB) as renewable energy sources through the gasification process. In this study, a downdraft gasifier was used to investigate the effect of process parameters on gas composition produced from gasification of EFB. The output concentrations and input parameters of EFB were studied using a response surface methodology with central composite design (CCD). The results showed that the optimal output conditions were at 4.7 L/min airflow rate and 363°C temperature for CO; 1.3 L/min airflow rate and 363°C temperature for CO_2; 1.3 L/min airflow rate and 726.42°C for CH_4; 1.3 L/min airflow rate and 900°C for H_2 and 1.3 L/min airflow rate and 900°C for H_2/CO. It can be concluded that production of syngas from EFB using downdraft gasifiers is promising to enhance green energy supplies in the future.

Keywords: *Empty fruit bunch; Gasification; Response surface methodology; Central composite design; Syngas; Downdraft.*

1. Introduction

The adverse effects of fossil fuel on the environment have pushed policy makers to consider renewable energies such as solar, wind, geothermal, hydro, biomass, tidal, and wave as alternative energy sources [1-2]. To exploit the enormous benefits of renewable energy sources, different countries proposed the use of biomass for the energy sectors [3-4]. In this regard, palm oil industries have been observed to have a big potential in the countries where the production is significant [5-6]. Palm oil sector generates a huge amount of waste from its plantation and milling activities. It was estimated that 195.8 million tons of biomass, on a wet basis, were generated every year from plantation and milling activities in Malaysia, the world's second largest producer and exporter of palm oil. Energy generated from the palm oil industry could utilize 82% of the total biomass wastes [7]. In recent years, huge replantation activity, expanding mill capacity and improvement on palm oil exchange rate have expanded the opportunity to utilize palm oil wastes as renewable energy sources. In the massive production of palm oil, the solid wastes such as empty fruit bunch (EFB), fruit fibers (FF), and palm kernel shell (PKS) are leftovers, which could be used as feedstocks to produce clean energies using different conversion processes [8]. EFB is a by-product of Fresh Fruit Bunch (FFB) following the removal of the nut. The presence of a high amount of fixed carbon content makes EFB to

be a potential renewable energy source. Pradeepkumar *et al.* [9] reported that 23% EFB could be generated from one tone of fresh fruit bunches milling process. It was highlighted that the amount of EFB generated from the total plantation area is tremendous, projecting significant contributions in clean energy generation ahead [10].

Palm trees have highest oil yields when compared with other oil crops such as soybean, sunflower, rapeseed with an enhanced ratio of 10:1 [11]. From the palm tree, Empty fruit bunch (EFB) has the highest sugar content, making it suitable to produce bio-ethanol through pyrolysis and fermentation or hydrolysis. Moisture, ash, volatile matter, inorganic elements, structural constituents, calorific value, particle size, and density are of great importance in understanding the changes that occur in the chemical structure of EFBs [12]. Mohammed *et al.* [13] conducted an experiment to characterize EFB. The proximate analysis was performed as per ASTM E 1756-01 standard test method. It was observed that EFB has a calorific value of 17.02 MJ/kg, with C, H, N, S and O contents of 46.62, 6.45, 1.21, 0.035, and 45.66 wt% db, respectively.

Nowadays gasification is considered as one of the best viable options to generate useful fuel gas from biomass wastes [14-15]. Gasification utilizes carbonaceous feedstocks such as coal, petro-coke or biomass to generate producer gases or syngas consisting of hydrogen, carbon monoxide, carbon dioxide, methane, and traces of other gases under oxygen-starved and high temperature conditions [16-18]. The process of gasification involves the reaction of carbon with air, oxygen, steam, carbon dioxide or a mixture of the gases at about 700°C or higher to produce gaseous products that can be used to generate electric power, heat or a raw material for the synthesis of chemicals, liquid fuels, or other gaseous fuels such as hydrogen [19].

The composition of the producer gas depends on several factors such as gasification temperature, oxidizing agent, reactor type, and feedstock type to mention few [20-22]. The gasifier type also influences the range of applicability of thermal inputs. Fixed-bed gasifiers are applicable for smaller units within the range of 10 to 10000 kW; fluidized-bed type is for intermediate units within the range of 5 to 100 MW; and entrained-flow gasifiers are used for large-capacity units of above 50 MW [20, 23]. Fixed bed gasifiers are classified into three types according to the gas flow direction in the gasifier. The residence time of the fuel in the fixed bed gasifiers is long with lower gas velocity [24]. The feedstocks move downward by the gravity force, and subsequently the bulk density of the feedstock should be high enough for continuous flow of the fuel during the gasification process. Hence, fixed bed gasifiers are more suitable only for sized feedstock with sufficient bulk density [7].

Gasifying EFB would also produce syngas that could potentially be utilized for power generation [25]. Moreover, the by-product of EFB after gasification could be used as key mediator in the chemical industry to produce methanol, dimethyl ether, and methyl tertbutyl ether. In this line, an experimental design approach is required for a parametric study and to provide models that can predict response variables as one at a time experimental approach would be difficult to get adequate information of syngas under the influences of multiple operating factors. However, there have been limited experiments performed to analyze the effects of operating factors on the response variables of syngas produced from the EFB. The objective of this study was, therefore, to investigate the effects of main operating factors on the EFB syngas production and develop predictive models through response surface method. This would help interrelate input factors with response variables and outcome fundamental conclusions.

2. Experimental setup and techniques

2.1. Feedstock preparation

In this study, Empty Fruit Bunch was utilized as a feedstock in the gasification experiment. Feedstock preparation involves characterization and gasification experiments. A fresh EFB weighing approximately 10 kg was collected from the palm oil mill, which was chopped down 3 to 5 inches size. Initially the feedstock was sun dry for 2 to 3 days to remove excess moisture. To remove the high hygroscopic moisture, the feedstock was dried in the oven at a temperature of 105°C for 24.0 hours as per ASTM E871-82 [26]. The dried EFB was then

shredded using strong granulator WSGP-230. A shredded EFB was sieved to particle size varying from 3 to 6 mm.

2.2. Design of experiment (DOE)

A response surface methodology is usually performed to handle complex experiments so that the interactions and their individual input factors effects on the response data could be achieved using fewer experiments. This offers less time and efforts to understand the experiments using DOE [27-28]. Moreover, it analyzes and reports the combined effects of input factors on the output variables as opposed to the conventional method in which one factor needs to be understood at a time, costing time and energy together [29-30].

In the current work, a response surface methodology (RSM) with central composite design (CCD) was used to design the experiment and analyze the results. A sequence of gasification experiment plans was generated considering temperature, airflow rate, and reaction time as input factors. The upper and lower limits of the input factor were determined based on the technical limitations of the experimental set-up and preliminary experiment results. From the experimental results functional correlations between the input and output parameters were developed to analyze the effect of input parameters on output parameters. From the preliminary experiment results the airflow rate was determined to be in the range of 2 L/min and 4 L/min. To ensure the safety of the gasifier, the temperature ranges were set between 500°C and 900°C. The reaction time in the ranges of 20 minutes to 40 minutes were considered. Table 2 shows the input factor of the experiment points of upper limits, lower limits, and mean values. In total, 17 experiments were conducted with 3 replicates at the center value. The replicated experiments help to estimate the errors and check the lack-of-fit of the experimental results [31].

In normal circumstances, first- or second-order polynomials were used to estimate the correlation, and the coefficients of the model were found using least-squares fit with the experimental data. Because the interactions between variables are important for this study, the CCD method of experimental design, which is the most common design to fit second-order polynomials, was used to predict the non-linear interactions between parameters [32]. Table 1 shows the input factors in uncoded units and their corresponding operating levels.

Table 1. Low, mean and upper values of the input factors

Input factor	Symbol	Lower value	Mean value	Upper value
Airflow rate (L/min)	x_1	2	3	4
Temperature (°C)	x_2	500	700	900
Reaction time (min)	x_3	20	30	40

2.3. Experiment setup

An externally heated downdraft fixed bed gasifier was used to perform experiments. The temperature of the gasifier was controlled by the power supply of the furnace using the portable heater controller. The gas composition data was analyzed by using X-stream (Emerson, Germany) gas analyzer. The gas analyzer measures the volumetric percentage of H_2, CO, CH_4, and CO_2. Once the gasifier reached the required temperature (500°C, 700°C, 900°C) 100 g of dry EFB fed to the gasifier from the top of the gasifier. The syngas was taped from the bottom of the gasifier, and it was cooled down in the gas cleaning and conditioning system to a temperature of ±4°C before it was delivered to the gas analyzer to ensure the supply of dry gas to the analyzer. Figure 1 shows the experimental setup. At the end of each experiment the gasifier was cleaned and ashes were removed for the consecutive experiment.

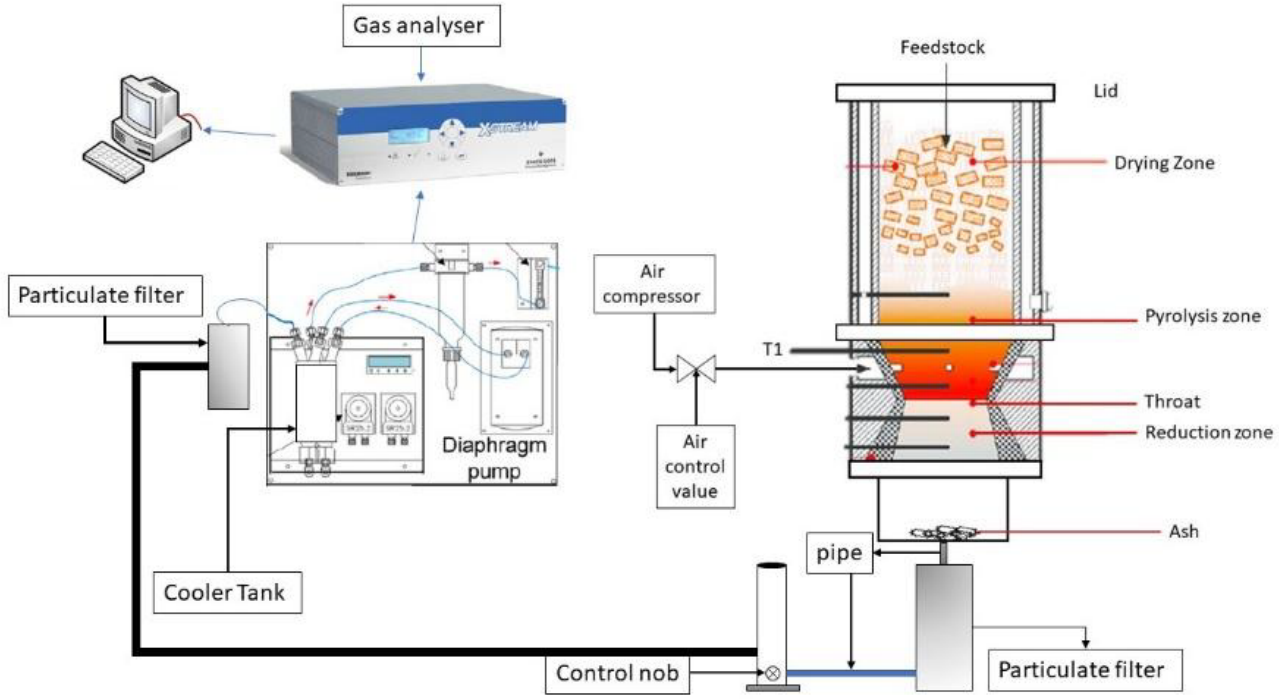

Figure 1. Experiment setup

3. Results and discussion

Based on the experimental design, the experiments were performed with three input parameters. A total of 17 experiments were carried out and four output parameters, i.e., H_2, CO, CH_4, and CO_2 were collected. From the outputs the ratio H_2/CO was calculated as the proportion of H_2 and CO is often required to evaluate the syngas for various applications. The output gases CO, CO_2, CH_4 and H_2 varied from 16.36 to 27.2, 20.71 to 49.84, 6.77 to 21.61, and 0.72 to 34.61 vol.%, respectively. H_2/CO ratio ranges from 0.017 to 1.209. A typical gas profile of four gases (vol.%) as a function of reaction time is depicted in Figure 2.

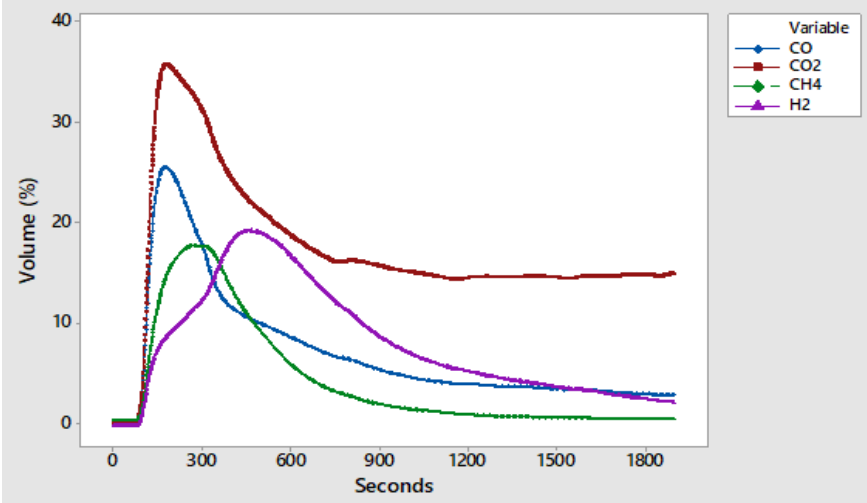

Figure 2. Gas profiles as a function of time during the gasification of EFB at 700°C, 3 L/min airflow rate, and 30 min reaction time

Table 2 shows the volumetric concentration of the gases obtained from the gasification as per design matrix of RSM CCD.

Table 2. Experimental results of CO, CO_2, CH_4, H_2 (vol.%) as per design matrix of CCD

Run	Temperature (°C)	AFR (L/min)	Reaction Time (min)	CO	CO_2	CH_4	H_2	H_2/CO
1	900	4.0	40	22.18	27.46	18.26	24.96	1.125
2	700	4.7	30	25.04	34.07	17.64	18.65	0.745
3	500	2.0	40	25.23	49.84	15.62	10.76	0.426
4	500	4.0	20	22.38	44.61	12.44	4.31	0.193
5	700	1.3	30	16.36	28.41	21.61	29.79	1.821
6	900	3.0	30	22.17	28.04	12.64	29.79	1.343
7	700	3.0	30	25.56	35.85	17.79	19.30	0.755
8	700	3.0	47	18.74	32.82	13.00	16.50	0.880
9	700	3.0	30	25.56	35.84	17.80	19.30	0.755
10	363	3.0	30	22.25	42.37	6.77	0.72	0.032
11	900	2.0	40	22.17	28.62	19.01	34.61	1.561
12	700	3.0	13	16.97	33.57	14.21	20.39	1.202
13	900	2.0	20	27.20	20.71	13.23	34.50	1.268
14	700	3.0	30	18.74	32.82	13.00	16.48	0.879
15	500	4.0	40	22.38	44.61	12.44	4.31	0.193
16	900	4.0	20	22.01	28.31	18.10	30.31	1.377
17	500	2.0	20	25.23	49.84	15.62	10.76	0.426

R^2 values for CH_4, H_2 and H_2/CO were 80.01%, 98.98% and 90.08% respectively, as shown in Table 3. Moreover, the variations were observed to be smaller for most of the runs conducted, and this indicates the precision of the model developed and predicted results as reported in [29]. The Adj-R^2 values for CH_4, H_2 and H_2/CO were 54.31%, 97.66% and 77.33%, respectively. The Adj-R^2 for H_2 and H_2/CO were close towards the prediction. The Adj-R2 value for CH_4 shows a lower percentage compared to the predicted value. As there were a huge number of secondary reactions occurring during the gasification process influencing the yield of CH_4 in various ways, the acquired Adj-R^2 in the forecast of H_2/CO was fairly sufficient [33]. The corresponding p-value of the coefficients evaluates the significance of each of the coefficients [34]. The combined effects of linear terms, square terms and interaction terms on the model were also evaluated under analysis of variance. The coefficients with p-value less than 0.05 were considered in the regression equation with 95% confidence level [35]. It was stated that coefficients with p-values less than 10% could also be considered in the model with 90% confidence limit [36]. In addition, the closeness between the R^2 and adj-R^2 values showed that there was no possibility of including non-significant terms in the regression models [37-38]. Residual errors and lack of fit were also insignificant as a high F-value and very small probability values lower than 0.05 were observed [39-40].

An assumption was made on the residual as it was normally and independently distributed for all the models of experiment with 0 mean value and constant variance [32]. Figures 3-5 show the residual plots of CH_4, H_2 and H_2/CO, respectively. As the normal probability plots approximately follow a straight line in the residual plots of Figs. 3a, 4a and 5a, the test shows that the assumption of normal distribution is valid. In Figure 3b & 3d - 5b & 5c the standardized residuals versus the fitted values and the standardized residuals versus the order of the data are scattered randomly, suggesting that the variance of the original observations are constant for all values of the responses [41].

Table 3. Response surface quadratic model evaluation table for coded variables of CO, H_2 and H_2/CO by Minitab.

Term	CH_4		H_2		H_2/CO	
	sum of square (ss)	p-value	sum of square (ss)	p-value	sum of square (ss)	p-value
Coefficient evaluation						
Constant	15.60	0.000	18.415	0.000	0.829	0.000
x_1	21.958	0.091	1382.100	0.000	2.445	0.000
x_2	5.841	0.346	151.410	0.000	0.501	0.024
x_3	1.107	0.673	10.200	0.090	0.018	0.599
x_1x_1	28.137	0.062	0.000	0.983	0.035	0.470
x_2x_2	35.399	0.042	37.280	0.007	0.016	0.142
x_3x_3	1.858	0.587	0.840	0.590	0.013	0.663
x_1x_2	13.758	0.165	0.110	0.843	0.003	0.841
x_1x_3	4.409	0.409	3.430	0.291	0.000	0.959
x_2x_3	3.947	0.434	3.730	0.273	0.037	0.461
ANOVA						
Model	160.403	0.074	1622.630	0.001	3.833	0.009
Linear	28.905	0.091	1185.610	0.000	2.965	0.002
square	81.927	0.041	42.190	0.424	0.237	0.345
2-way Interaction	22.113	0.351	7.270	0.905	0.039	0.881
Residual						
Lack of fit	24.790	0.699	13.100	0.572	0.412	0.060
Pure error	15.290		5.300		0.010	
Total	200.482		1796.130		4.255	
Coefficient of determination						
R^2	80.01%		98.98%		90.08%	
Adj-R^2	54.31%		97.66%		77.33%	

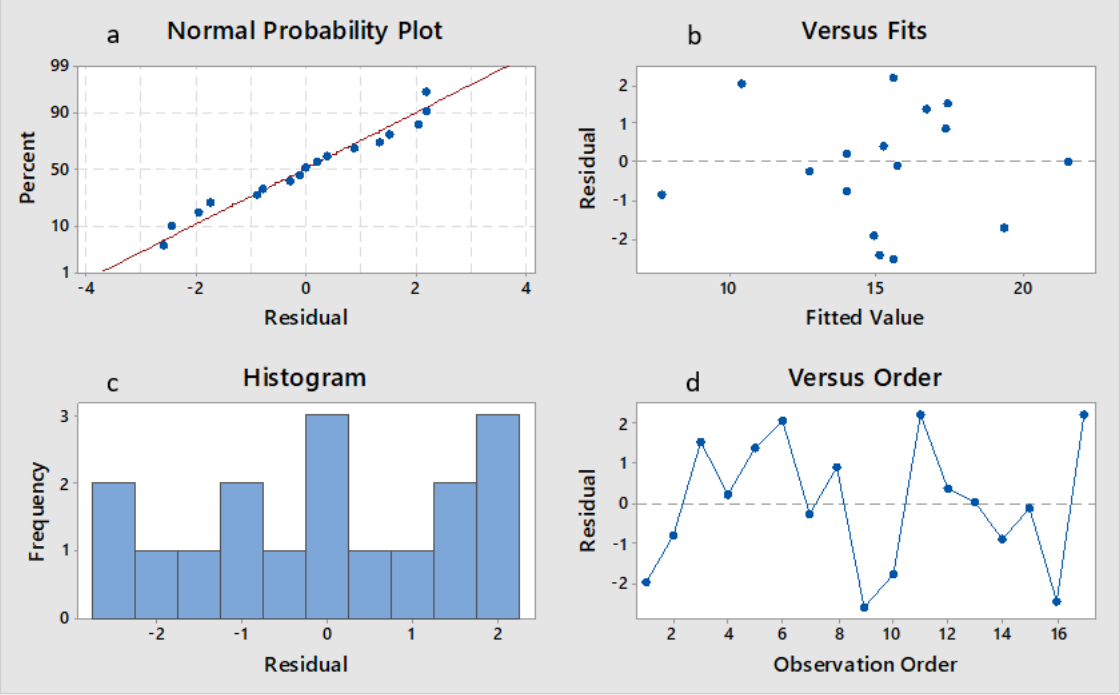

Figure 3. Residual plot of CH_4: (a) Residual vs Percentage, (b) Fitted value vs Residual, (c) Residual vs Frequency, (d) Observation order vs Residual

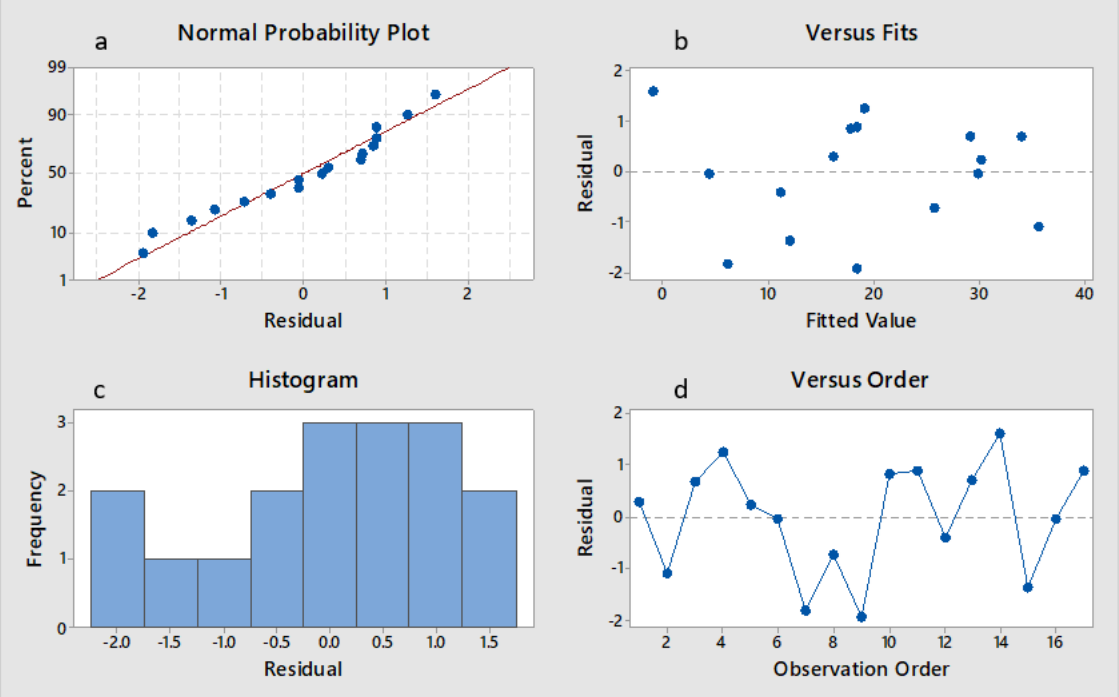

Figure 4. Residual plot for H_2: (a) Residual vs Percentage, (b) Fitted value vs Residual, (c) Residual vs Frequency, (d) Observation order vs Residual

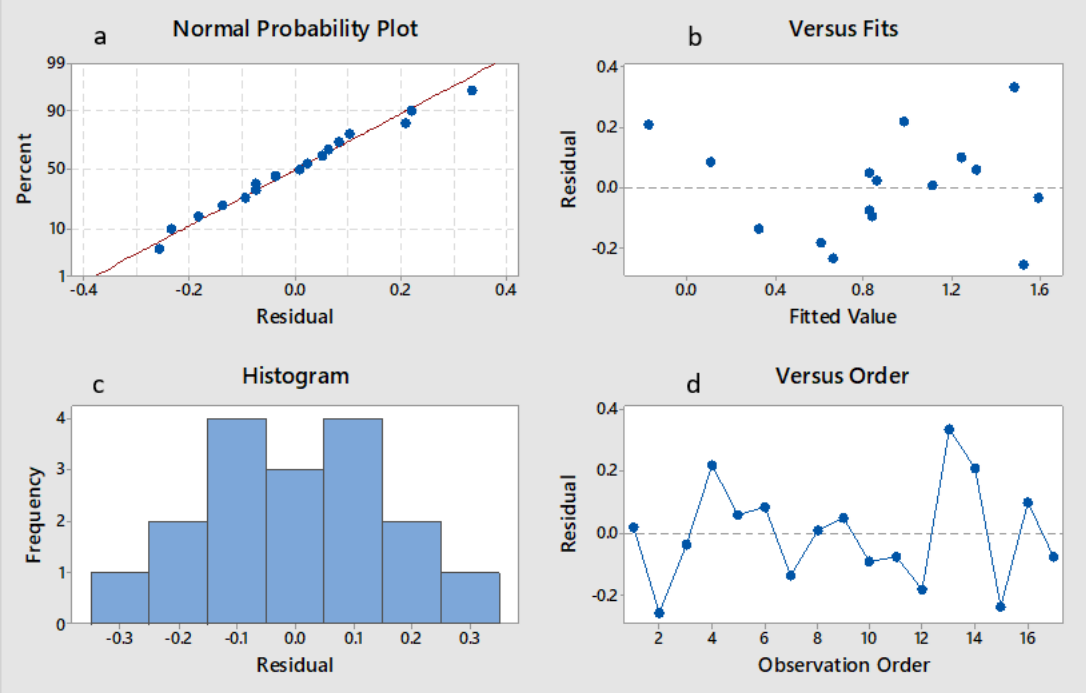

Figure 5. Residual plot for H_2/CO: (a) Residual vs Percentage, (b) Fitted value vs Residual, (c) Residual vs Frequency, (d) Observation order vs Residual.

To develop the model equations for the response variables, a second order polynomial regression equations were used with the regression coefficients of the natural (un-coded) units. Following the evaluation of the significance of the coefficients in the model, the equation could be deduced to the simplified form [27]. However, different research works stated that

the full quadratic equation is sufficient and preferred to precisely predict the response variables [42-43]. The developed models of the response variables with the full second order polynomial equations are given as follows. The model equations 1 to 3 are predictive equations for CH_4, H_2 and H_2/CO, respectively.

$$CH_4 = 14.9 + 0.0442x_1 - 13.3x_2 + 0.212x_3 - 0.000048x_1^2 + 1.694x_2^2 - 0.00388x_3^2 + 0.00656x_1x_2 + 0.000371x_1x_3 - 0.0702x_2x_3 \quad (1)$$

$$H_2 = -10.2 + 0.0692x_1 - 11.28x_2 + 0.504x_3 - 0.00x_1^2 + 1.738x_2^2 - 0.0026x_3^2 - 0.00059x_1x_2 - 0.000327x_1x_3 - 0.00683x_2x_3 \quad (2)$$

$$\frac{H_2}{CO} = -0.06 + 0.0046x_1 - 0.744x_2 - 0.0041x_3 - 0.000002x_1^2 + 0.1155x_2^2 + 0.000318x_3^2 + 0.00009x_1x_2 + 0.000002x_1x_3 - 0.00676x_2x_3 \quad (3)$$

3.1. Effect of input factors on response variables

3.1.1. Effect of input factor on CH_4 output

Figures 6 and 7 show a contour plot and 3D surface plot of CH_4 against the combined effect of temperature, air flow rate and reaction time. The purpose of plotting contour plot and 3D plot was to determine the interaction effect of input factor on each response variable. In Figure 6, contour plot and surface plot determine an output variable response of CH_4 against two input factors such as temperature and reaction time by maintaining airflow rate as third input factor at lower, mean and upper values. The dots indicate the experimental parameters and the prediction lines were drawn accordingly based on the derived second order polynomial equation.

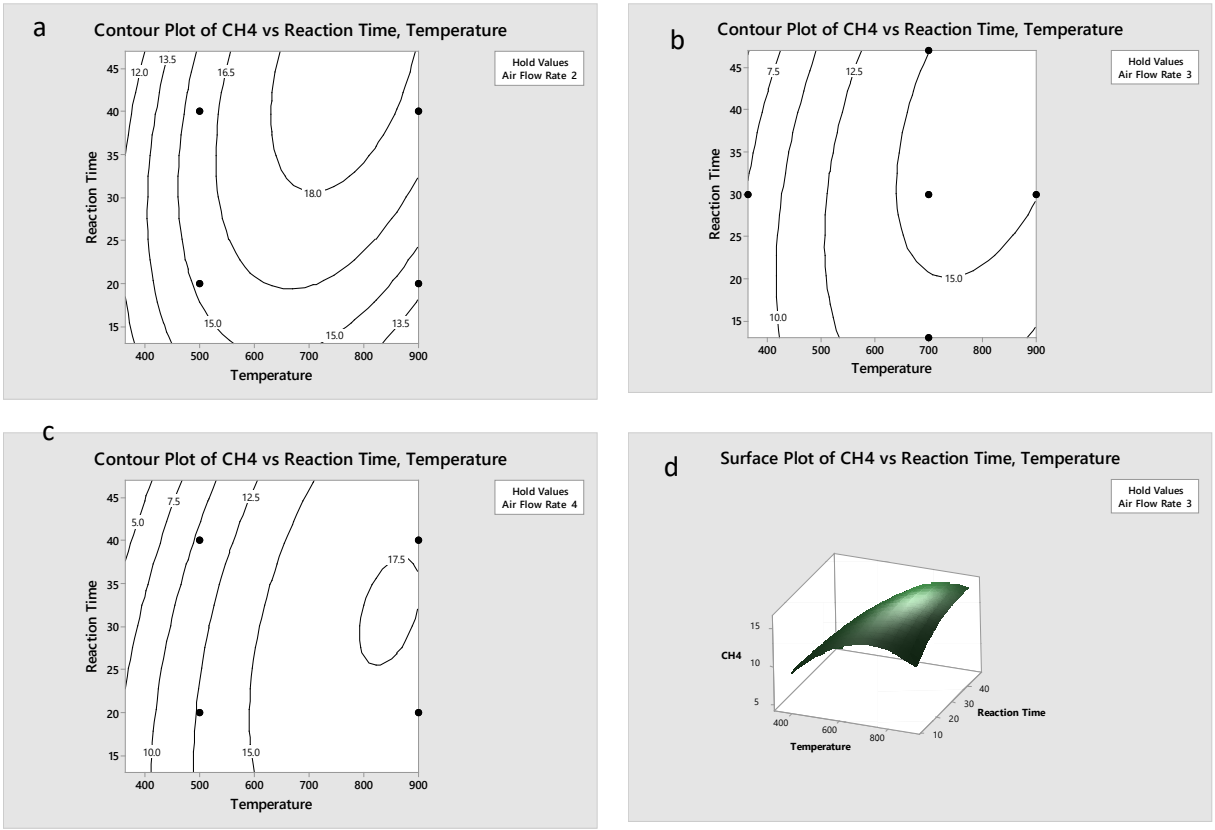

Figure 6. Contour Plot and surface plot of CH_4 at different flow rates: (a) 2 L/min, (b) 3 L/min (c) 4 L/min (d) 3D surface plot at 3 L/min airflow rate

CH_4, in Figure 6a-d, reacted frequently at the temperature ranges of approximately 600°C - 900°C and above 30 minutes with the airflow rate of 2 L/min where the maximum value was 18%, as shown in Figure 6a. Within the same condition, the minimum values were 12% at 400°C and 35 minutes. For the condition of 3 L/min airflow rate, the maximum CH_4 value was 15% at the temperature ranges from 650°C - 900°C after 20 minutes. As for the minimum values of 2.5% were encountered at approximately 400°C, as shown in Figure 6b. When the airflow rate increased to 4 L/min, it showed a maximum value of 17.5% at the temperatures within 800°C -900°C. Combined effects of reaction time and temperature showed that CH_4 yield was high at low temperature. CH_4 yield increased as temperature increased to 700ºC, after which temperature had marginal effect on CH_4 yield. For 3 L/min airflow rate, the CH_4 yield was shifted to low at high temperature. A similar observation was observed at 4L/min airflow rate. This effect was due to the forward methanation reaction of ($CO_2 + 4H_2 \leftrightarrows CH_4 + 2H_2O$ - 165 kJ/mol) which is more active at low temperature range; as the temperature increased the reaction turns to char gasification ($C + 3H_2 \leftrightarrows CH_4 + H_2O$ -206 kJ/mol). However, at high temperature and high airflow rate of 3 L/min and 4 L/min the overall Ch_4 yield was smaller marginally. Because of the high air flow rate along with high temperature, CH_4 breaks down into CO and H_2 causing a slight decrease in CH_4.

Figure 7a-d shows the CH_4 yield against temperature and air flow rate with constant reaction time. The maximum values 20 vol.% of CH_4 were obtained at the temperature of 700°C and airflow rate of above 4.5 L/min. As airflow rate increased at low temperature the CH_4 yield dropped and reached to 10 vol.% at airflow rate of 2.5 L/min and temperature of above 400ºC, as can be seen in Figure 7a. However, in Figure 7c, the CH_4 of 20 vol.% maximum point was obtained in the condition of 1.5L/min airflow rate and temperatures between 450°C and 900°C. Whereas in Figure 7b, the maximum values of CH_4 were 20% and it was obtained in 2 conditions which were 500°C -850°C at airflow rate of 1.5 L/min and 700°C with airflow rate of 4.5 L/min and above. Therefore, the maximum CH_4 was obtained at a temperature of 726°C and 3 L/min airflow rate with the concentration of 23.02 vol.%.

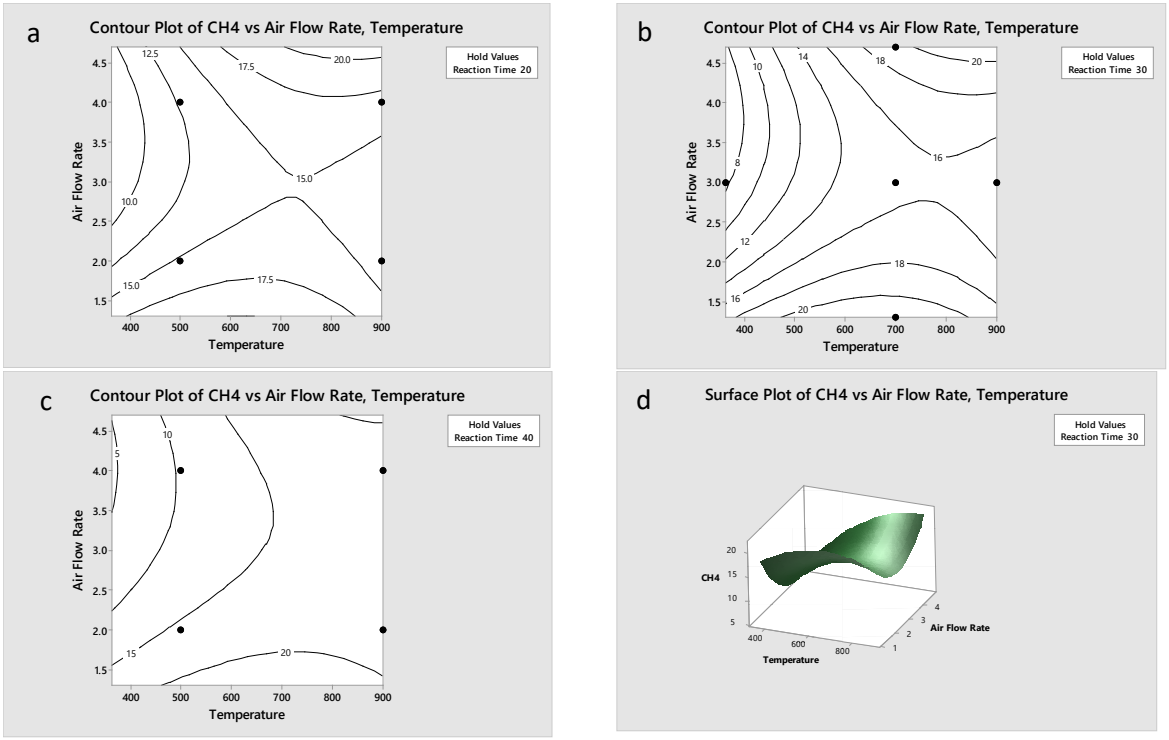

Figure 7. Contour plot and surface plot of CH_4 at different reaction time: (a) 20 min (b) 30 min (c) 40 min, (d) 3D surface plot at 30 min reaction time

3.1.2. Effect of input factors on H_2 output

Figures 8 and 9 show the combined effect of input factors on H_2 yields. The H_2 yield has an increasing trend with temperature of the gasification in the range from 400ºC to 900ºC. A 30 vol.% or higher concentrations of H_2 were produced at high temperature with low airflow rates. The concentration of H_2 approximately increased by 5 vol.% when the airflow rate was 2 L/min compared to 3 L/min and 4 L/min airflow rates. However, in this condition the reaction time requires more time to maintain the concentration value of H_2 and prevent lack of oxidation reaction as the temperature is required to perform endothermic reaction towards H_2 [20].

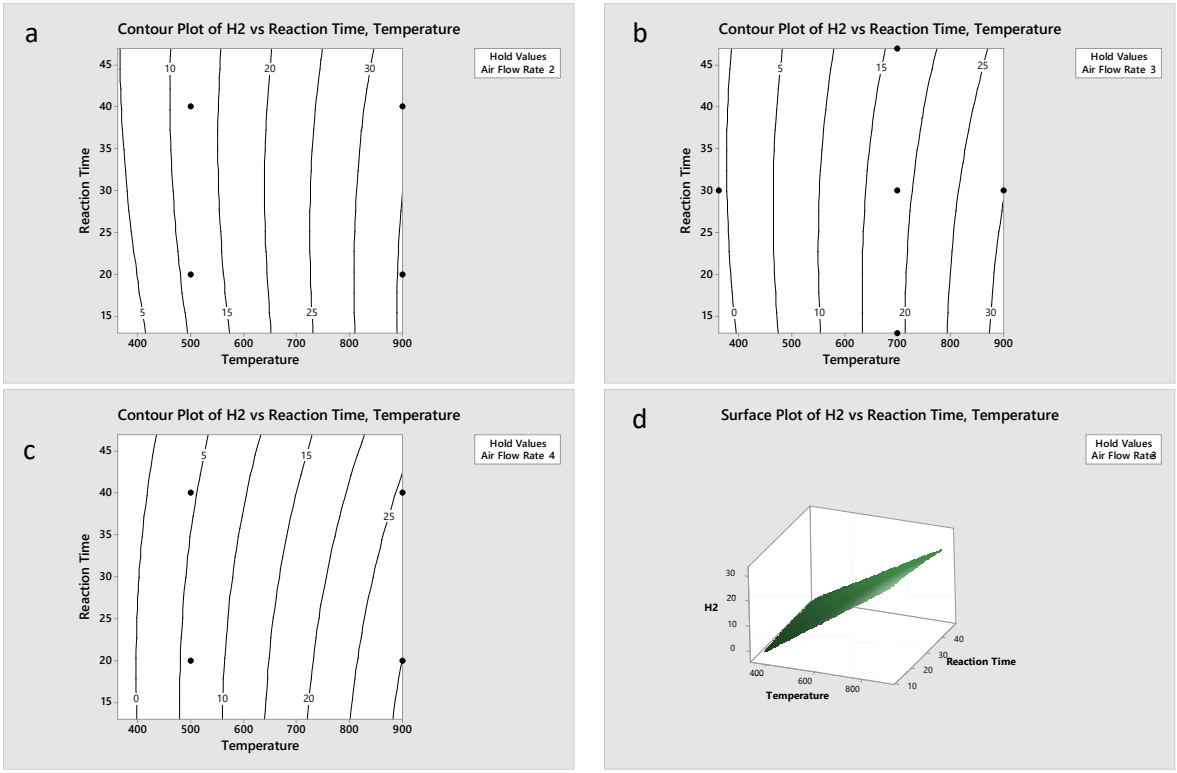

Figure 8. Contour Plat and surface plot of H_2 at different flow rates: (a) 2 L/min (b) 3 L/min (c) 4 L/min, (d) 3D surface plot at 3 L/min air flow rate

The combined effect of airflow rate and temperature on H_2 yield is depicted in Figure 9. It was observed that the temperature increased H_2 production over the temperature of 900ºC.

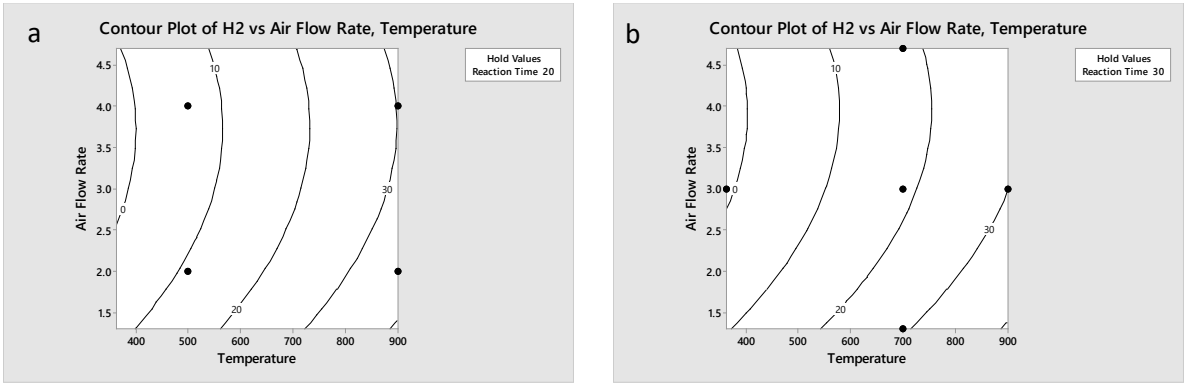

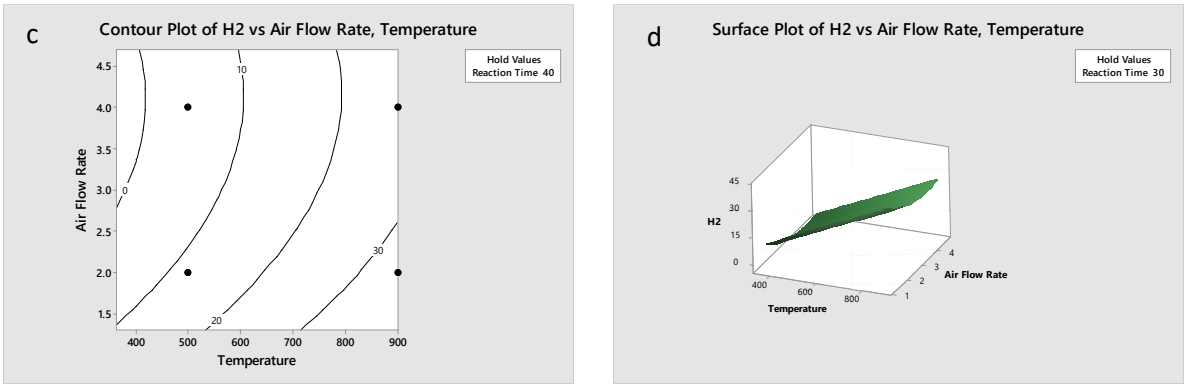

Figure 9. Contour plot and surface plot of H_2 at different reaction time: (a) 20 min, (b) 30 min, (c) 40 min, (d) 3D surface plot at 30 min reaction time

H_2 yield increased as airflow rate increased to 3.5 L/min at any temperature. The airflow rate above 3.5 L/min decreased the H_2 production because of the excess air that decreases H_2 production and increases CO_2 yield, eventually turning gasification into mild combustion. The maximum H_2 concentration was 30% at temperature above 700°C with the maximum airflow rate of 3 L/min. When airflow rate was above 3 L/min, the concentration of H_2 decreased by 10% with the temperature. Therefore, optimization concentration of H_2 was 40.19% at the temperature of 900°C with 1.3 L/min airflow rate.

3.1.3. Combined effect of input factors on H_2/CO ratio

The combined effects of temperature, airflow rate, and reaction time on the H_2/CO ratio are shown in Figures 10 and 11.

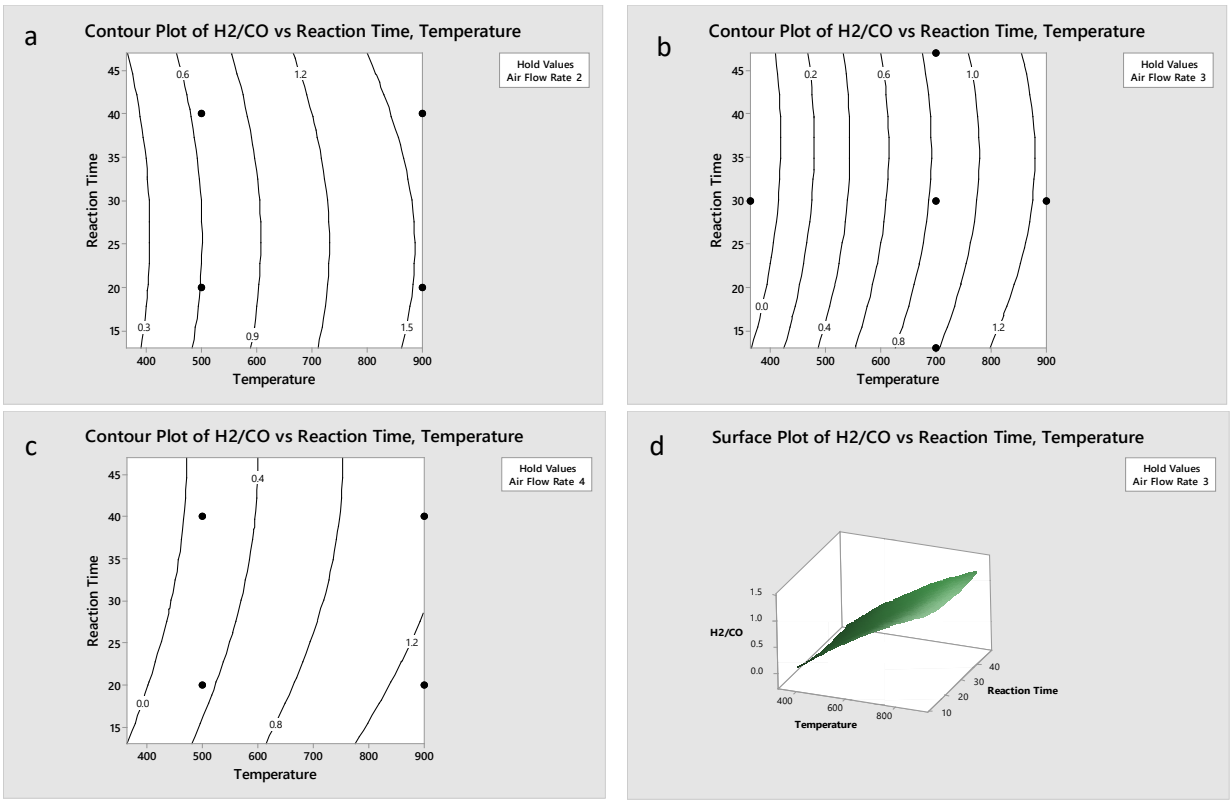

Figure 10. Contour Plat and surface plot of H_2/CO at different air flow rates: (a) 2 L/min, (b) 3 L/min (c) 4 L/min, (d) 3D surface plot at 3 L/min

b

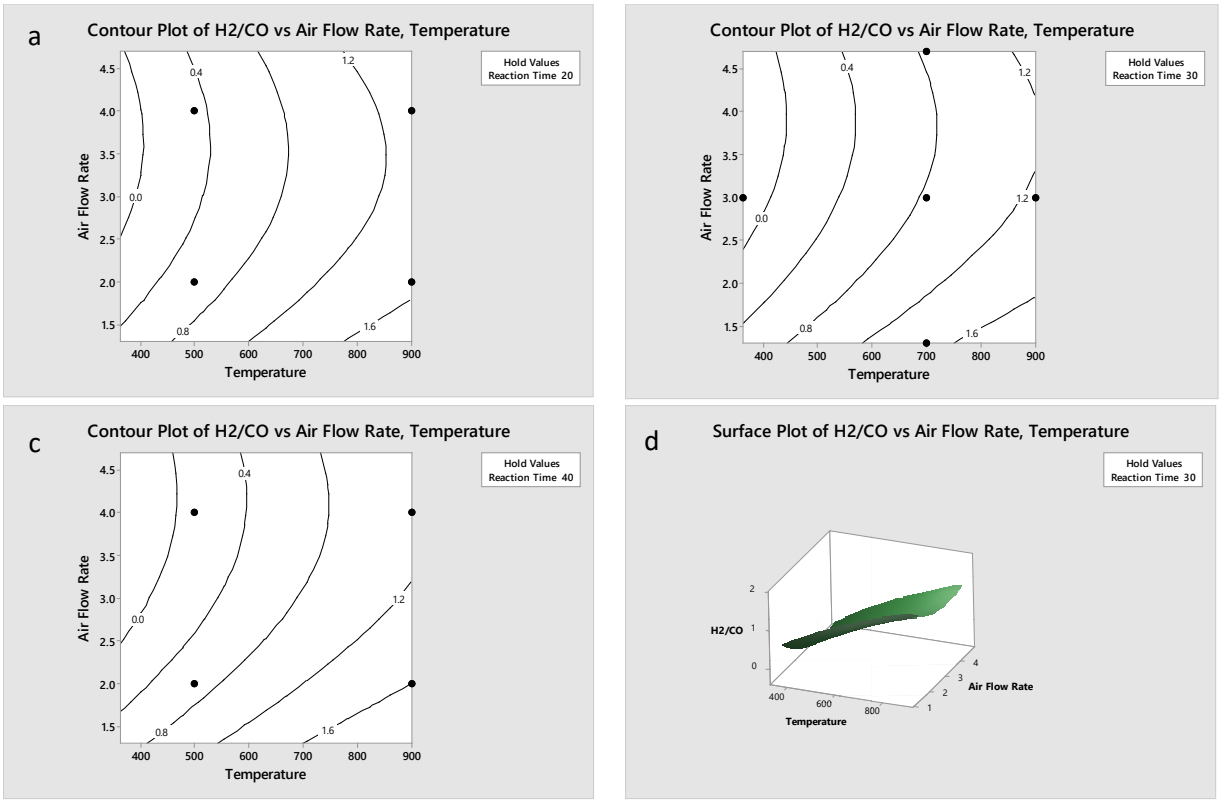

Figure 11. Contour plot and surface plot of H_2/CO at different reaction time (a) 20 min, (b) 30 min, (c) 40 min, (d) 3D surface plot at 30 min reaction time

The ratio of H_2/CO shows a maximum concentration of 1.6% and above when temperature reaches 900°C at flexible reaction time with constant airflow rate of 2 L/min as shown in Figure 10a. As the airflow rate increases the concentration of H_2/CO reduces 4%. Therefore, a high temperature and lower airflow rate gave maximum output. As for the maximum concentration of 2.102% H_2/Co ratio, it was obtained at 900°C with the airflow rate of 1.3 L/min.

3.1.4. Optimization of input operating factor

Table 4 shows optimal outputs for input factors.

Table 4. Optimization of gasification process of EFB

Output	Input		Optimal output		
	Name	Optimal condition	Prediction	Experiment	Variation
CO	Airflow rate Temperature	4.7 (L/min) 363 (°C)	33.16	25.92	7.24 (28%)
CO_2	Airflow rate Temperature	1.3 (L/min) 363 (°C)	67.1	55.6	11.5 (20.6%)
CH_4	Airflow rate Temperature	1.3 (L/min) 726.42 (°C)	26.7	23.02	3.68 (16%)
H_2	Airflow rate Temperature	1.3 (L/min) 900 (°C)	42.72	40.82	1.90 (4.6%)
H_2/CO	Airflow rate Temperature	1.3 (L/min) 900 (°C)	2.549	2.102	0.447 (21%)

To maximize the overall output yields, the input conditions were to be set at 542°C with 1.3 L/min, at which output concentrations were 21.10, 20.00, 43.16, and 22.22 for CH_4, H_2, CO_2, and CO respectively. Optimized airflow rate was at 1.3 L/min except for CO where it

required 4.7 L/min air flow rate to be optimal condition. In regard to temperature, the optimal condition ranged from 363°C to 900°C. For instance, CO required 38 minutes, H_2 required 23 minutes and CO_2 and CH_4 required 47 minutes on its own optimal condition. Therefore, output optimal variations were 7.24 (28%), 11.5 (20.6%), 3.68 (16%), 1.90 (4.6%) and 0.447 (21%) for CO, CO_2, CH_4, H_2 and H_2/CO, respectively.

3.1.5. Model verification

To validate the prediction results a verification was performed using R^2 as shown in Figure 12. A linear line corresponding to the experimental and prediction results was drawn. This approach was capable of indicating tab acceptable fit results between the operating factors of temperature, airflow rate and reaction time against the response variables. R^2 of the gasification processes are required to be greater than 0.9 as the points were near to the linear line [44]. Accordingly, it was observed that the R^2 values, for H_2 and H_2/CO, were higher than 0.9.

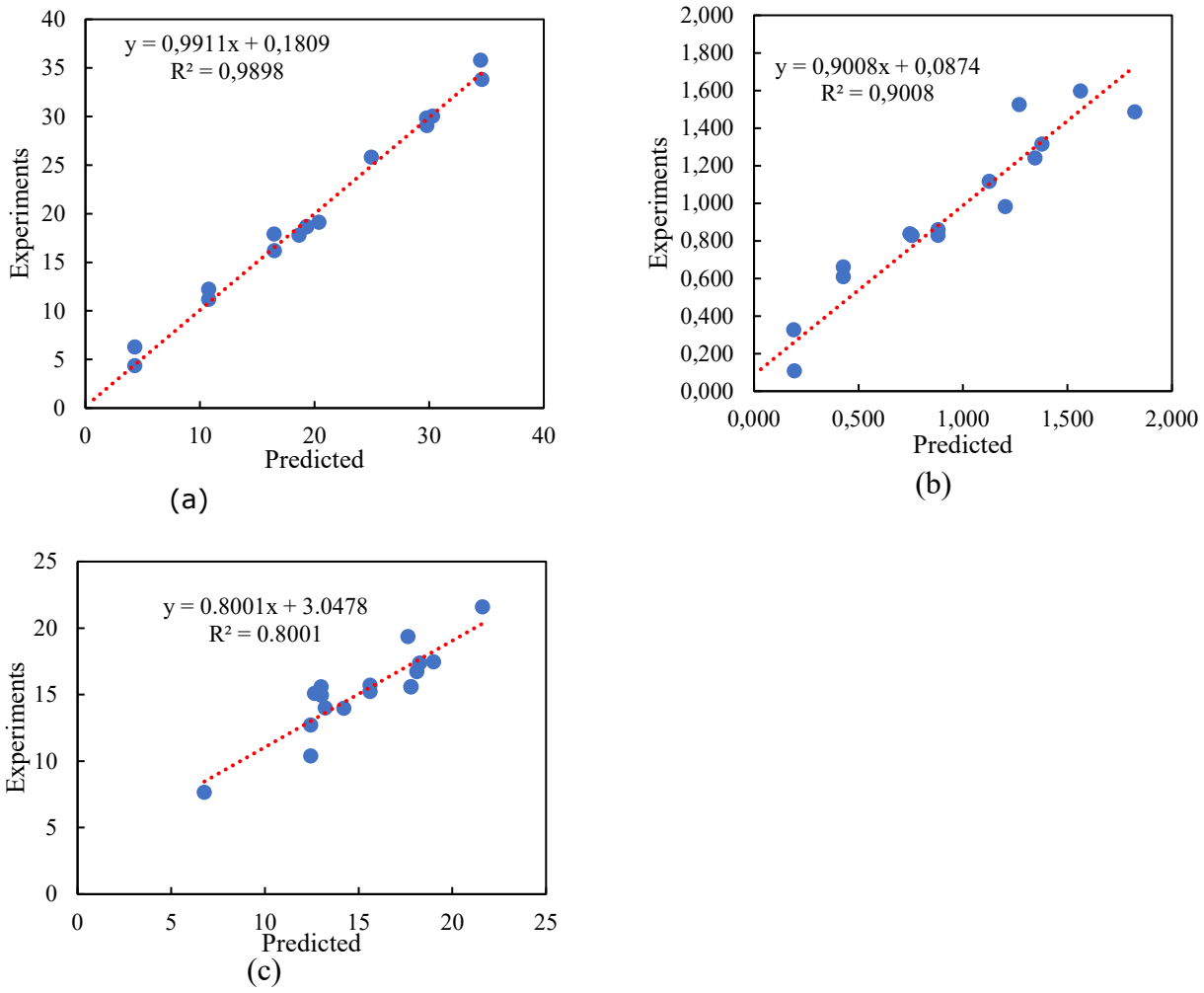

Figure 12. Predicted versus experimental results for (a) H_2 (b) H_2/CO (c) CH_4

4. Conclusion

This paper presents gasification of empty fruit bunch (EFB) for the syngas production. A downdraft gasifier was used to investigate the effect of input factors on syngas composition. Input parameters and response variables of EFB were investigated using a response surface

methodology (RSM) with central composite design (CCD). It was observed that the input parameters such as temperature and air flow rates have an influence on response variables of empty fruit bunch. The optimal output conditions were at 4.7 L/min airflow rate and 363°C temperature for CO; 1.3 L/min airflow rate and 363°C temperature for CO_2; 1.3 L/min airflow rate and 726.42°C for CH_4; 1.3 L/min airflow rate and 900°C for H_2 and 1.3L/min airflow rate and 900°C for H_2/CO. Using downdraft gasifier, the syngas composition of EFB such as H_2, H_2/CO and CH_4 had high R^2 values of 0.9898, 0.9008 and 0.8001, respectively, indicating the accuracy of the models developed. It can be concluded that production of syngas from EFB using downdraft gasifiers is promising and could take part in the green energy supplies in the future.

Acknowledgement

The authors would like to thank Universiti Teknologi PETRONAS for the experimental facilities provided.

References

[1] Chala G, Abd Aziz A, Hagos F. Natural Gas Engine Technologies: Challenges and Energy Sustainability Issue. Energies 2018;11.
[2] Chala GT, Ma'Arof M, Sharma R. Trends in an increased dependence towards hydropower energy utilization-A short review. Cogent Engineering 2019:1631541.
[3] Inayat M, Sulaiman SA, Kurnia JC, Naz MY. Catalytic and noncatalytic gasification of wood–coconut shell blend under different operating conditions. Environmental Progress & Sustainable Energy 2019;38:688.
[4] Chala GT, Guangul FM, Sharma R. Biomass Energy in Malaysia-A SWOT Analysis. 2019 IEEE Jordan International Joint Conference on Electrical Engineering and Information Technology (JEEIT): IEEE; 2019, p. 401.
[5] Hock TK, Chala GT, Cheng HH. An innovative hybrid steam-microwave sterilization of palm oil fruits at atmospheric pressure. Innovative Food Science & Emerging Technologies 2020;60:102289.
[6] Sukiran MA, Abnisa F, Daud WMAW, Bakar NA, Loh SK. A review of torrefaction of oil palm solid wastes for biofuel production. Energy Conversion and Management 2017;149:101.
[7] Guangul F, Sulaiman S, Ramli A. Gasification of oil palm fronds with preheated inlet air. Malaysia: Universiti Teknologi PETRONAS 2013.
[8] Juturu V, Wu JC. Production of high concentration of l-lactic acid from oil palm empty fruit bunch by thermophilic Bacillus coagulans JI12. Biotechnology and applied biochemistry 2018;65:145.
[9] Pradeepkumar T. Management of horticultural crops: New India Publishing; 2008.
[10] Derman E, Abdulla R, Marbawi H, Sabullah MK. Oil palm empty fruit bunches as a promising feedstock for bioethanol production in Malaysia. Renewable energy 2018;129:285.
[11] Karmakar A, Karmakar S, Mukherjee S. Properties of various plants and animals feedstocks for biodiesel production. Bioresource Technology 2010;101:7201.
[12] Omar R, Idris A, Yunus R, Khalid K, Isma MA. Characterization of empty fruit bunch for microwave-assisted pyrolysis. Fuel 2011;90:1536.
[13] Mohammed M, Salmiaton A, Azlina WW, Amran MM. Gasification of oil palm empty fruit bunches: A characterization and kinetic study. Bioresource technology 2012;110:628.
[14] Basu P. Biomass gasification, pyrolysis and torrefaction: practical design and theory: Academic press; 2018.
[15] Pandey B, Prajapati YK, Sheth PN. Recent progress in thermochemical techniques to produce hydrogen gas from biomass: a state of the art review. International Journal of Hydrogen Energy 2019;44:25384.
[16] Dou B, Zhang H, Song Y, Zhao L, Jiang B, He M, et al. Hydrogen production from the thermochemical conversion of biomass: issues and challenges. Sustainable Energy & Fuels 2019;3:314.
[17] Shahbaz M, Al-Ansari T, Inayat M, Sulaiman SA, Parthasarathy P, McKay G. A critical review on the influence of process parameters in catalytic co-gasification: Current performance and challenges for a future prospectus. Renewable and Sustainable Energy Reviews 2020;134:110382.
[18] Inayat M, Sulaiman SA, Kurnia JC, Shahbaz M. Effect of various blended fuels on syngas quality and performance in catalytic co-gasification: A review. Renewable and Sustainable Energy Reviews 2019;105:252.

[19] Inayat M, Sulaiman SA, Shahbaz M, Bhayo BA. Application of response surface methodology in catalytic co-gasification of palm wastes for bioenergy conversion using mineral catalysts. Biomass and Bioenergy 2020;132:105418.
[20] Guangul FM, Sulaiman SA, Ramli A. Gasifier selection, design and gasification of oil palm fronds with preheated and unheated gasifying air. Bioresource Technology 2012;126:224.
[21] Sulaiman SA, Roslan R, Inayat M, Naz MY. Effect of blending ratio and catalyst loading on co-gasification of wood chips and coconut waste. Journal of the Energy Institute 2018;91:779.
[22] Khor K, Lim K, Alimuddin ZZ. Laboratory-scale pyrolysis of oil palm trunks. Energy Sources, Part A: Recovery, Utilization, and Environmental Effects 2010;32:518.
[23] Basu P. Biomass gasification and pyrolysis: practical design and theory: Academic press; 2010.
[24] Rajvanshi AK. Biomass gasification. Alternative energy in agriculture 1986;2:82.
[25] Chala GT, Lim YP, Sulaiman SA, Liew CL. Thermogravimetric analysis of empty fruit bunch. MATEC Web of Conferences: EDP Sciences; 2018, p. 02002.
[26] Inayat M, Sulaiman SA, Inayat A, Shaik NB, Gilal AR, Shahbaz M. Modeling and parametric optimization of air catalytic co-gasification of wood-oil palm fronds blend for clean syngas (H2+CO) production. International Journal of Hydrogen Energy 2020.
[27] Myers R, Montgomery D, Anderson-Cook C. Response surface methodology: process and product optimization using designed experiments . New Jersey: A John Wiley & Sons. Inc; 2009.
[28] Montgomery DC, Runger GC. Applied statistics and probability for engineers: John Wiley & Sons; 2010.
[29] Montgomery DC. Response surface methods and other approaches to process optimization. Design and analysis of experiments 1997.
[30] Inayat M, Sulaiman SA, Kurnia JC. Catalytic co-gasification of coconut shells and oil palm fronds blends in the presence of cement, dolomite, and limestone: Parametric optimization via Box Behnken Design. Journal of the Energy Institute 2019;92:871.
[31] Myers RH, Montgomery DC, Vining GG, Borror CM, Kowalski SM. Response surface methodology: a retrospective and literature survey. Journal of quality technology 2004;36:53.
[32] Karimipour S, Gerspacher R, Gupta R, Spiteri RJ. Study of factors affecting syngas quality and their interactions in fluidized bed gasification of lignite coal. Fuel 2013;103:308.
[33] Guangul FM, Sulaiman SA, Ramli A. Study of the effects of operating factors on the resulting producer gas of oil palm fronds gasification with a single throat downdraft gasifier. Renewable Energy 2014;72:271.
[34] DeCoursey W. Statistics and probability for engineering applications: Elsevier; 2003.
[35] Montgomery DC. Experimental design for product and process design and development. Journal of the Royal Statistical Society: Series D (The Statistician) 1999;48:159.
[36] Liu J, Hu H, Xu J, Wen Y. Optimizing enzymatic pretreatment of recycled fiber for improving its draining ability using response surface methodology. BioResources 2012;7:2121.
[37] Sauter RM. Introduction to probability and statistics for engineers and scientists. Taylor & Francis; 2005.
[38] Fermoso J, Gil MV, Arias B, Plaza M, Pevida C, Pis J, et al. Application of response surface methodology to assess the combined effect of operating variables on high-pressure coal gasification for H2-rich gas production. International Journal of Hydrogen Energy 2010;35:1191.
[39] Khuri AI, Mukhopadhyay S. Response surface methodology. Wiley Interdisciplinary Reviews: Computational Statistics 2010;2:128.
[40] Ahnazarova SL, Kafarov VV, Rep'ev AP. Experiment optimization in chemistry and chemical engineering: Mir Publishers; 1982.
[41] Carley KM, Kamneva NY, Reminga J. Response surface methodology. Carnegie-Mellon Univ Pittsburgh Pa School of Computer Science; 2004.
[42] Nasrollahzadeh H, NAJAFPOUR GD, Aghamohammadi N. Biodegradation of phenanthrene by mixed culture consortia in batch bioreactor using central composite face-entered design. 2007.
[43] Gupta S, Kulahci M, Montgomery DC, Borror CM. Analysis of signal–response systems using generalized linear mixed models. Quality and reliability engineering international 2010;26:375.
[44] Raheem A, Ji G, Memon A, Sivasangar S, Wang W, Zhao M, et al. Catalytic gasification of algal biomass for hydrogen-rich gas production: Parametric optimization via central composite design. Energy Conversion and Management 2018;158:235.

To whom correspondence should be addressed: Dr. Girma T. Chala, International College of Engineering and Management, Muscat, Oman, E-mail: irma@icem.edu.om